



Published in final edited form as:

*Acc Chem Res.* 2020 October 20; 53(10): 2273–2285. doi:10.1021/acs.accounts.0c00402.

## Development of Triggerable, Trackable and Targetable Carbon Monoxide Releasing Molecules

Livia S. Lazarus<sup>1</sup>, Abby D. Benninghoff<sup>2</sup>, Lisa M. Berreau<sup>1</sup>

<sup>1</sup>Department of Chemistry & Biochemistry, Utah State University, 0300 Old Main Hill, Logan, UT 84322-0300

<sup>2</sup>Department of Animal, Dairy and Veterinary Sciences, Utah State University, 4815 Old Main Hill, Logan, UT 84322-4815

### Conspectus

Carbon monoxide (CO) is a gaseous signaling molecule produced in humans via the breakdown of heme in an O<sub>2</sub>-dependent reaction catalyzed by heme oxygenase enzymes. A long-lived species relative to other signaling molecules (e.g., NO, H<sub>2</sub>S), CO exerts its physiological effects via binding to low-valent transition metal centers in proteins and enzymes. Studies involving the administration of low doses of CO have shown its potential as a therapeutic agent to produce vasodilation, anti-inflammatory, anti-apoptotic, and anti-cancer effects. In pursuit of developing tools to define better the role and therapeutic potential of CO, carbon monoxide releasing molecules (CORMs) were developed. To date, the vast majority of reported CORMs have been metal carbonyl complexes, with the most well-known being Ru<sub>2</sub>Cl<sub>4</sub>(CO)<sub>6</sub> (CORM-2), Ru(CO)<sub>3</sub>Cl(glycinate) (CORM-3), and Mn(CO)<sub>4</sub>(S<sub>2</sub>CNMe(CH<sub>2</sub>CO<sub>2</sub>H)) (CORM-401). These complexes have been used to probe the effects of CO in hundreds of cell- and animal-based experiments. However, through recent investigations, it has become evident that these reagents exhibit complicated reactivity in biological environments. The interpretation of the effects produced by some of these complexes is obscured by protein binding, such that their formulation is not clear, and by CO leakage and potential redox activity. An additional weakness with regard to CORM-2 and CORM-3 is that these compounds cannot be tracked via fluorescence. Therefore, it is unclear where or when CO release occurs, which confounds the interpretation of experiments using these molecules. To address these weaknesses, our research team has pioneered the development of metal-free CORMs based on structurally-tunable extended flavonol or quinolone scaffolds. In addition to being highly controlled, with CO release only occurring upon triggering with visible light (photoCORMs), these CO donors are trackable via fluorescence prior to CO release in cellular environments and can be targeted to specific cellular locations.

In the Account, we highlight the development and application of a series of structurally-related flavonol photoCORMs that: (1) sense characteristics of cellular environments prior to CO release; (2) enable evaluation of the influence of cytosolic versus mitochondrial-localized CO release on cellular bioenergetics; (3) probe the cytotoxicity and anti-inflammatory effects of intracellular versus extracellular CO delivery; and (4) demonstrate that albumin delivery of a photoCORM

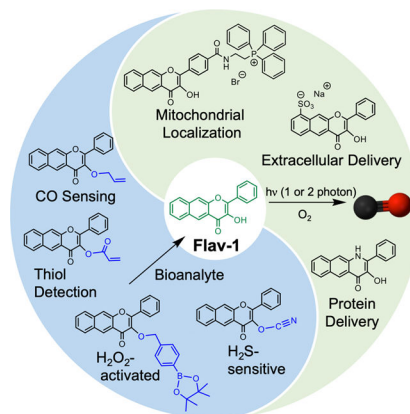
---

Corresponding author lisa.berreau@usu.edu.

The authors declare no competing financial interest.

enables potent anti-cancer and anti-inflammatory effects. A key advantage of using triggered CO release compounds in these investigations is the ability to examine the effects of the molecular delivery vehicle in the absence and presence of localized CO release, thus providing insight into the independent contributions of CO. Overall, flavonol-based CO delivery molecules offer opportunities for triggerable, trackable, and targetable CO delivery that are unprecedented in terms of previously reported CORMs and, thus, offer significant potential for applications in biological systems.

## Graphical Abstract



## I. Introduction

Despite its reputation as a toxic molecule, carbon monoxide (CO) is now recognized as a beneficial small molecule in humans. CO is generated via the oxidative degradation of heme catalyzed by heme oxygenase enzymes (Figure 1).<sup>5</sup> CO is the most long-lived among the three major known gasotransmitters (H<sub>2</sub>S, NO and CO). CO exhibits its biological effects through coordination to low-valent transition metal centers in proteins. This chemistry is involved in several essential biological functions, including the regulation of ion channels<sup>6,7</sup> and intracellular signaling pathways,<sup>8</sup> which results in cardioprotective,<sup>9</sup> anti-inflammatory,<sup>10</sup> anti-apoptotic,<sup>11</sup> and anti-cancer<sup>12</sup> effects. Therefore, CO is of significant current interest as a potential therapeutic for treating a variety of conditions<sup>13</sup>, with several clinical trials involving low dose CO gas as a therapy for inflammation and blood vessel function completed or underway.<sup>14</sup>

CO-releasing molecules (CORMs) were developed as an approach toward advancing the therapeutic potential of CO, as well as to improve the research tools available to probe the role of CO in biology. First generation CORMs were simple metal carbonyl complexes that release CO spontaneously in aqueous environments.<sup>15</sup> The CORMs that have been most commonly applied in biological studies are [RuCl<sub>2</sub>(CO)<sub>3</sub>]<sub>2</sub> (CORM-2),<sup>16</sup> [Ru(CO)<sub>3</sub>Cl(glycinate)] (CORM-3),<sup>17</sup> and [Mn(CO)<sub>4</sub>{S<sub>2</sub>CNMe(CH<sub>2</sub>CO<sub>2</sub>H)}] (CORM-401).<sup>18</sup> As transition metal complexes, these CORMs are susceptible to ligand exchange in biological environments, which can result in CO leakage and the formation of protein adducts.<sup>19</sup> Lacking any fluorescent components, the location of CORM-2, CORM-3,

or CORM-401 cannot be tracked in biological environments, thus leaving the site of CO delivery unclear. Recent studies have also provided evidence that CORM-2 and CORM-3 can act as reductants and exhibit redox reactivity involving the Ru(II) fragment remaining following CO release.<sup>20,21</sup> This reactivity complicates the interpretation of the observed biological effects produced upon CO delivery from these CORMs. A comparative investigation of CO delivery to heme proteins from CORM-2, CORM-3, and CORM-401 also provided evidence that the presence of the metal complexes or their CO release byproducts can interfere with biological assays.<sup>22</sup> Many metal-carbonyl CORMs have been developed, including examples in which CO delivery is controlled through triggered release using visible light (photoCORMs),<sup>23</sup> enzyme activity (ETCORMs),<sup>24</sup> or magnetic heating,<sup>25</sup> as well as examples for which the CO release agent or product can be tracked via fluorescence.<sup>26</sup> However, the inherent presence of a transition metal remains the challenge. This issue has led to the incorporation of CORMs into materials so as to sequester the metal ion both prior to and following the CO release reaction.<sup>27</sup>

To avoid the challenges associated with using transition metal-containing CORMs in biological systems, a few laboratories initiated studies into the development and evaluation of organic CO donors. CO-releasing structural motifs employed in the preparation of spontaneous donors include boronocarbonates<sup>28</sup> and norbornadiene-7-one derivatives.<sup>29</sup> The latter compounds are actively being developed as tunable spontaneous CO release agents for therapeutic applications.<sup>30–32</sup> Visible light-triggered organic photoCORMs have been constructed using cyclic diketones,<sup>33</sup> xanthene carboxylic acid,<sup>34</sup> and meso-carboxy BODIPY<sup>35</sup> structural motifs. Notably, very few organic CORMs that exhibit fluorescence properties making them trackable in cells are currently known.<sup>31,33,36</sup>

A current challenge in CORM development is targeted CO delivery to specific biological sites. Metal carbonyl CORM derivatives have been reported with: 1) peptide, polymer or biotin conjugates for targeted delivery to tumors,<sup>37,38</sup> 2) oxidatively sensitive appendages for triggered CO release in cancer cells,<sup>39</sup> and/or 3) incorporation in nanomaterials to enable targeting to malignant tumors via the EPR effect.<sup>40</sup> In terms of metal-free CORMs, only one report of mitochondrial-targeted delivery of CO has been published using a spontaneous CO-releasing framework.<sup>31</sup> Thus, targeted delivery of CO using a metal-free organic CORM remains largely undeveloped.

In this Account we outline the development of extended flavonol and quinolone frameworks as novel metal-free CORMs for visible light-triggered CO delivery. The intrinsic properties of these frameworks demonstrate a versatility that is unprecedented in metal-free CORMs reported to date. These properties include: 1) clean, quantitative CO release reactivity resulting in the formation of a single fully characterized, non-toxic organic byproduct; 2) trackable fluorescence in cells prior to CO release; and 3) structural amenability to achieve targeted delivery. Potent biological effects using these delivery vehicles demonstrated via *in vitro* and *in vivo* disease models suggest significant potential for these systems in advancing understanding of the role CO in biological systems.

## II. Extended Flavonol and Quinolone PhotoCORM Frameworks

Flavonols are naturally occurring compounds found in many fruits and vegetables. Quercetin, an abundant flavonol in the human diet, has been extensively evaluated for its potent anti-inflammatory, antioxidant and anticancer properties.<sup>41,42</sup> Quercetin is known to undergo dioxygenase-type CO release in bacteria and fungi.<sup>43</sup> The core framework of quercetin, 3-hydroxyflavone, has been reported to release CO thermally and/or photochemically under UV-light illumination conditions.<sup>44</sup>

Rationalizing that extension of the aromatic framework via incorporation of an additional fused ring would lead to visible light absorbing flavonols, we prepared **1** (Figure 2) via the Algar-Flynn-Oyamada reaction in ~60% yield.<sup>45</sup> Compound **1** undergoes clean, quantitative, visible light-induced CO release in a range of solvents, including cell media, to give a single non-toxic (up to 100  $\mu\text{M}$  in A549 cells) depside product (**2**).<sup>1,45</sup> We note that this reaction is similar to the heme oxygenase-mediated CO release from heme as both are dioxygenase-type processes. The quantum yield for CO release from **1** in  $\text{CH}_3\text{CN}$  under 419 nm light illumination and air is 0.007(1) with  $\phi_e = 43$ . Notably, two-photon laser excitation ( $\lambda_{\text{ill}} = 800 \text{ nm}$ ) produces the same CO release reaction.<sup>46</sup> Compound **1** exhibits a fluorescent emission at ~580 nm allowing the molecule to be tracked in the green channel prior to CO release in cells and zebrafish (Figure 1).<sup>45,46</sup> This photoCORM distributes cytosolically in a range of cells, exhibiting mild cytotoxicity in A549 cells ( $\text{IC}_{50} = 81 \mu\text{M}$ ).<sup>45</sup> Compound **1** binds weakly to bovine serum albumin (BSA,  $K_a = 3.2 \times 10^3 \text{ M}^{-1}$ ) at the warfarin binding site.<sup>1</sup> Visible light-induced CO delivery from **1** in RAW 264.7 cells produces significant anti-inflammatory effects as evidenced by >50% TNF- $\alpha$  suppression starting at 1  $\mu\text{M}$  compound concentration.<sup>47</sup> Notably, in the absence of CO release, **1** also produces >50% TNF- $\alpha$  reduction starting at 25  $\mu\text{M}$ . This observation indicates that the inherent anti-inflammatory properties of the flavonol framework can contribute to the bioactivity of the photoCORM.

Klan and co-workers examined the mechanism of the visible light-induced,  $\text{O}_2$ -dependent CO release reaction of **1** using steady-state and transient absorption spectroscopy and quantum mechanical calculations.<sup>48</sup> Three CO release pathways were identified for the acid-base forms of **1** (Scheme 1). The triplet excited tautomer of the neutral flavonol ( $^3\text{1Z}^*$ ) as well as the triplet excited state of the conjugate base of **1** ( $^3\text{1B}^*$ ) undergo reaction with  $^3\text{O}_2$  leading to the release of CO and depside formation. The ground state conjugate base of **1** (**1B**) also undergoes efficient reaction with  $^1\text{O}_2$  leading to CO release and depside formation.

The 3-hydroxybenzo[*g*]quinolone **3** (Figure 3(a)) was previously reported as a dye.<sup>49</sup> Visible light illumination of an acetonitrile solution of **3** was found to quantitatively produce depside and CO with a quantum yield of 0.0045(1) and  $\phi_e = 33$ .<sup>2</sup> Fluorescence visualization of **3** in cells was successful only in the presence of bovine serum albumin (BSA) which facilitates the aqueous solubility and uptake of **3**. Notably, **3** has a 900-fold greater affinity for BSA ( $K_a = 2.9 \times 10^6 \text{ M}^{-1}$ ) than does **1**. Visible light-induced CO release from the **3**:BSA conjugate produces a potent anticancer ( $\text{IC}_{50} = 24 \mu\text{M}$ ) effect in A549 cells, which may be due to the albumin-facilitated accumulation of **3** in the cells.<sup>50</sup> CO release from **3** at 80 nM also produces complete suppression of lipopolysaccharide (LPS)-induced TNF- $\alpha$  production

in RAW 264.7 murine macrophage cells. This potent anti-inflammatory effect is unprecedented among photoCORMs reported to date.<sup>2</sup> Similar to **1**, the quinolone framework also exhibits anti-inflammatory effects (>50% TNF- $\alpha$  suppression at 10  $\mu$ M) in the absence of CO release.

Compounds **1** and **3** represent prototype frameworks for the development of families of visible light-triggered CO-releasing molecules. The clean, quantitative CO release induced by visible light, the fluorescence trackability of the compounds in cells, and the inherent bioactivity of the frameworks provide a starting point for the development of novel CO donors with enhanced functionality.

### III. Environment Sensing Prior to Triggered CO Release

Analyte sensing is important for detecting pathological conditions, which are often characterized by aberrant concentrations of various biomarkers, such as oxidative stress as indicated by perturbed levels of reactive oxygen or sulfur species (ROS and RSS, respectively). With the long-term goal of developing molecules to deliver an optimal supply of CO to biological targets to address oxidative stress, we and others initiated the development of multifunctional flavonol-based photoCORMs possessing environment sensing capability. These molecular structures operate via Boolean logic gates (Scheme 2) with sequence-activated outputs triggered by distinct stimuli (e.g., bioanalyte, light and O<sub>2</sub>). This approach affords a unique and reproducible molecular behavior for intelligent recognition.<sup>51–53</sup>

Addition of a sensing component to **1** is achieved via functionalization of the 3-hydroxyl position, typically in a high yield, one-step reaction. This modification produces a significant blue-shift (~100 nm) in the absorption and emission features versus those exhibited by **1**, which enables independent tracking of the sensing compound via its blue emission prior to deprotection. In the sensor molecules studied to date (*vide infra*), the presence of a 3-OR substituent inhibits visible light-driven CO release reactivity, thus enabling sequential molecular AND logic gate (stimulus-triggered) reactivity using a variety of analyte sensing motifs (Scheme 2). Due to their increased lipophilicity, the sensor-appended compounds **4** and **7** exhibit better cellular uptake than **1** and therefore serve as a camouflaged form of the CO release compound.

#### Thiol Sensing Followed by CO Release

Assessment of biothiol levels as an indicator of oxidative stress was achieved via incorporation of a Michael acceptor in **4** (Scheme 2), the reactivity of which results in deprotection of the 3-OR moiety and the formation of **1**, which can then undergo visible light-triggered CO release.<sup>3</sup> Compound **4** reacts quickly with cysteine (Cys), but slower with homocysteine (Hcy) and glutathione (GSH). The enhanced rate of sensing reactivity with cysteine is due to the formation of a kinetically favored seven-membered ring which leads to carbon-oxygen bond cleavage and release of **1**.<sup>54</sup> The deprotection of **4** to produce **1** was found to proceed with a detection limit of 24 nM, which is comparable to previously published cysteine sensors.<sup>55</sup> Compound **4** is mildly cytotoxic (IC<sub>50</sub> = 62  $\mu$ M in A549 cells), but slightly less cytotoxic than **1** under identical conditions (IC<sub>50</sub> = 41.5  $\mu$ M).<sup>45</sup> Using

confocal microscopy, **4** showed good cellular uptake in A549 cells as indicated by intense intracellular blue emission (Figure 4). Importantly, **4** enabled detection of endogenous cellular biothiols after pretreatment of the cells with N-ethylmaleimide (NEM). This is evidenced by the appearance of the green intracellular emission of **1** after 1 h of incubation (Figure 4). Subsequent illumination of the cells with visible light under normoxic conditions (20% O<sub>2</sub>) for 10 min resulted in loss of green emission, consistent with the AND logic gate operation sequence and CO delivery. As cellular redox imbalance is often associated with hypoxia,<sup>56</sup> the efficiency of CO delivery from **1** was also evaluated under hypoxic (1% O<sub>2</sub>) conditions. Illumination of a DMSO:H<sub>2</sub>O (1:1, v:v) solution of **1** (25 μM) at 419 nm under 1% O<sub>2</sub> resulted in complete conversion to **2** in <1200 s.

The distinct chromatic switches between **4** and **1**, and subsequently **1** and **2**, couple the response to a biomarker with gasotransmitter molecular output in a sense-of-logic enabled photoCORM (SL-photoCORM). This molecule was the prototype for the development of additional environment-sensing flavonol derivatives for CO delivery.

### H<sub>2</sub>S Sensing Followed by CO Release

The maintenance of cellular homeostasis also involves a network of signaling molecules, including other gasotransmitters, such as H<sub>2</sub>S.<sup>57</sup> Notably, CO and H<sub>2</sub>S exhibit reciprocal regulation, with CO binding to the heme site of cystathionine-β-synthase resulting in enzyme inhibition and increased H<sub>2</sub>S generation from cysteine catalyzed by γ-cystathionase in a sequence termed heme-dependent metabolic track switching.<sup>58</sup> This sequence occurs under endoplasmic reticulum stress, conditions under which CO is generated from HO-1. O<sub>2</sub>-dependent CO/H<sub>2</sub>S interplay has also been reported in carotid bodies where CO production is linked to the regulation of H<sub>2</sub>S production in hypertension and sleep apnea.<sup>59</sup>

As an approach toward gaining insight into the potential interplay of CO and H<sub>2</sub>S in cellular environments, we developed a flavonol-based molecular tool to study their interaction.<sup>60</sup> The cyanate moiety of **5** (Figure 5) is highly responsive to H<sub>2</sub>S/HS<sup>-</sup> with high selectivity against common bioanalytes and a detection limit (79 nM) that is comparable to several previously reported H<sub>2</sub>S sensors.<sup>61</sup>

While the cyanate moiety of **5** was found to be hydrolytically unstable with respect to the formation of **1** in test tube fluorescence experiments in DMSO:water (1:1), cellular uptake of the compound minimizes this reactivity. Experiments performed in human umbilical vein endothelial cells (HUVECs) showed good cellular uptake of **5** as indicated by blue intracellular emission observed after 24 h of incubation (Figure 5). The absence of green emission in this experiment, which would indicate the presence of **1**, demonstrates the hydrolytic stability of **5** in cells. Exposure of the cells to H<sub>2</sub>S (10 μM) results in the disappearance of the blue emission and the appearance of the green emission of **1**. Visible light illumination results in loss of the latter signal, indicating CO release from **1**. Thus, similar to the biothiol sensor **4**, compound **5** operates via AND logic gates and is a viable molecular tool for further exploration of H<sub>2</sub>S/CO interplay in biology.

## H<sub>2</sub>O<sub>2</sub> Sensing Followed by CO Release

As an approach toward evaluating cellular oxidative stress via sensing of ROS prior to CO delivery, a flavonol–boronate conjugate (**6**, Scheme 2), was developed by Tang and co-workers.<sup>46</sup> In solution experiments, this molecule was shown to sense H<sub>2</sub>O<sub>2</sub> (DL = 66 nM) to produce **1**, which subsequently undergoes visible light-induced CO release via an AND logic gate sequence. Compound **6** is biocompatible for both *in vitro* and *in vivo* studies, exhibiting low cytotoxicity. The H<sub>2</sub>O<sub>2</sub>-sensing deprotection reaction of **6** and subsequent light-induced CO delivery from **1** in vascular smooth muscle live cells were confirmed via fluorescence studies and use of a CO-sensing fluorescent probe. Notably, **1** was shown to undergo two-photon induced CO release, with an absorption cross-section ( $\delta$ ) at 800 nm of 96 GM (1 GM = 10<sup>-50</sup> cm<sup>4</sup> s photon<sup>-1</sup>).

An aspect of cellular ROS regulation yet to be fully explored is related to H<sub>2</sub>O<sub>2</sub>-induced fluctuation produced upon administration of angiotensin II, a potent peptide hormone vasoconstrictor used in treating hypotension and hypovolemia. Considering that CO is a known vasorelaxant via several signaling pathways,<sup>62</sup> **6** was applied in an angiotensin II-treated transgenic line of zebrafish (Tg (flila: EGFP)) wherein the vascular endothelium was highlighted with green fluorescent protein (GFP). Upon administration of angiotensin II, vasoconstriction occurred with the vascular diameter decreasing by 32% (Figure 6), with H<sub>2</sub>O<sub>2</sub> upregulation being confirmed by an attenuation effect on this condition by *N*-acetyl-L-cysteine. The vasodilation effect of CO produced upon illumination of **6** using a two-photon laser (800 nm) was shown with the vascular diameter increasing to 23.8  $\mu$ M, which is comparable to the diameter in control animals (Figure 6).

## Analyte Replacement: CO Sense and CO Release

A notable absence in the rapidly expanding field of CO sensors are analyte replacement probes that can replenish the CO that is consumed during detection to avoid perturbing cellular homeostasis. As an initial approach toward addressing this deficiency, **1** was functionalized with an allyl ether tail to produce **7**. Compound **7** senses CO (delivered from CORM-2 or CO gas) via Pd(0)-mediated Tsuji-Trost type reactivity to generate **1** (Figure 7(right)) via an AND logic gate sequence.<sup>63</sup> In DMSO, **7** exhibits CO sensing with a fluorescence detection limit of 3.19  $\mu$ M. However, the use of PdCl<sub>2</sub> and CORM-2 in DMSO results in the formation metal complexes of **1** (e.g., [(**1**)Pd(CH<sub>3</sub>CN)<sub>2</sub>]<sup>+</sup> (detected by ESI-MS in CH<sub>3</sub>CN)) which limit subsequent visible light-driven CO release reactivity. Importantly, metal complexation in cells (HUVECs) is minimized such that both CO sensing and trackable visible light-induced CO release reactivity are feasible (Figure 7). Compound **7** is the first reported analyte replacement fluorescent sensor for CO.

## CO Delivery via a Tandem Light-Triggered Micelle

A carbon monoxide releasing polymer containing the extended flavonol motif (CORP, **8**) was generated via direct RAFT polymerization (Scheme 3).<sup>64</sup> This polymer produces self-assembled micelle amphiphiles with excellent water dispersity. CO release from **8** involves a cascade of two visible light-triggered photochemical reactions (**8** → **9** → **10**, Scheme 3). These chemical transitions are trackable via fluorescence, thus enabling self-reporting CO

release. A blue-to-red-to-no emission sequence is observed for this process, with the red emission being attributed to aggregated forms of the flavonol (**9**) within the micelle environment. Similar reactivity was found to occur in RAW 264.7 cells in which good cellular uptake was evident with no significant cytotoxicity (up to 0.2 g/L).

Injections of solutions of micellular nanoparticles of **8** (0.1 g/L) in BALB/c mice with subsequent illumination at 410 nm demonstrated the potential of **8** as a trackable, visible light-induced CO donor for the treatment of cutaneous wound diseases. A full-thickness cutaneous wound healing model showed that the CO delivery from **8** produced a faster wound healing rate compared to controls, especially after 7-day treatments (Figure 8), with **8** and CORM-3 exhibiting similar impacts on wound healing.

With this being the case, it is important to consider the ease of handling of the two CO delivery systems. Aqueous solutions of the triggered flavonol-based CO releasing molecules such as **1** and **8** are stable for several days under dark conditions. This contrasts with aqueous solutions of CORM-3 which have a limited half-life (~1 min; pH 7.4, 37 °C) and exhibit CO leakage, thus leading to uncertainty with regard to the amount of CO delivered.<sup>21</sup>

#### IV. Targeting

Localization of CORMs is of particular current interest to probe how the site of CO release relates to the biological signaling effects of this stable, diffusible gas molecule. The Ru(II) carbonyl CORMs used most extensively to date in biological studies (CORM-2<sup>16</sup> and CORM-3<sup>17</sup>) release CO spontaneously in aqueous environments, thus likely providing predominantly extracellular delivery, similar to delivery by CO gas. This extracellular delivery contrasts with the site of biological production of CO, which occurs as a part of heme degradation catalyzed by HO-1, an endoplasmic reticulum (ER)-localized enzyme with exposure to the cytosol under normal conditions. Notably, in the presence of stimuli (*e.g.*, heme, LPS, oxidants, hypoxia, etc.), HO-1 partially translocates to the mitochondria, nucleus, and caveolae.<sup>65</sup> This subcellular distribution of HO-1 under various conditions raises intriguing questions about organelle-specific effects of CO. To address these questions, CORMs that undergo triggered CO release while positioned at precise locations are needed. In this regard, the fluorescence trackable CO-releasing frameworks of **1** and **3** offer unique opportunities for investigation. Below, we outline three initial ways we have used these CORMs or derivatives thereof to probe biological questions regarding localized CO release.

##### Extra- Versus Intracellular CO Release

We have functionalized **1** to probe how extra- versus intracellular CO release affects CO-induced toxicity and anti-inflammatory effects.<sup>47</sup> Suspension of **1** in H<sub>2</sub>SO<sub>4</sub> at room temperature for 18 h produces **11** (Figure 9), a water-soluble version of the extended flavonol framework. This sulfonated flavonol exhibits similar spectroscopic and visible light-induced quantitative CO release reactivity to that of **1**. The increased water solubility of **11** prevents its cellular uptake, as evidenced by fluorescence studies in RAW 264.7 cells. This contrasts with **1** which has been identified as localizing in cytosol via fluorescence microscopy.<sup>45</sup> In terms of toxicity, both intracellular **1** and extracellular **11** are non-cytotoxic



in RAW 264.7 cells (up to 100  $\mu\text{M}$ ) prior to CO release and have non-cytotoxic organic byproducts. Notably, visible light-induced CO release from **1** was found to be significantly cytotoxic ( $\text{IC}_{50} = 22.39 \pm 2.98 \mu\text{M}$ ) whereas CO release from extracellular **11** (up to 100  $\mu\text{M}$ ) remained non-cytotoxic. These observations show that the location of CO release is important with regard to cytotoxicity. CO release from **1** and **11** was also evaluated in anti-inflammatory studies using LPS-challenged RAW 264.7 cells. Monitoring the suppression of TNF- $\alpha$  by **1**, **11**, and their organic CO release products (depsides) using an ELISA assay under dark and light conditions, we found that CO release suppressed TNF- $\alpha$  levels to a similar extent regardless of whether CO was delivered extra- or intracellularly. A reduction of >50% in TNF- $\alpha$  was found for **1** and **11** starting at 1  $\mu\text{M}$  and 0.04  $\mu\text{M}$ , respectively. Notably, the overall extent of TNF- $\alpha$  suppression from **1** and **11** depends on the scaffold of the CO delivery vehicle, with the pre-CO release scaffold of **11** enhancing TNF- $\alpha$  suppression at low nanomolar concentrations, while **1** provides anti-inflammatory effects at low micromolar concentrations. Such anti-inflammatory contributions of the flavonol framework are not surprising as naturally occurring flavonols are known to exhibit anti-inflammatory effects.<sup>66</sup> We note that the CO-release product depsides, whether illuminated and non-illuminated, did not produce significant TNF- $\alpha$  suppression.

### Mitochondrial-Targeted CO Release

Very little is currently known about the effect of targeted CO delivery to mitochondria, endoplasmic reticuli, or nuclei. This knowledge gap is primarily due to the lack of CORMs available for targeted, controlled intracellular delivery of CO. With regard to mitochondria, assessment of the effect of localized CO delivery on the reactivity of the heme centers of the electron transport chain and overall mitochondrial bioenergetics is particularly needed.

Wang and co-workers reported the first example of a mitochondria-localized CO delivery approach using a bioorthogonal reaction-based pair of compounds each containing a cationic triphenylphosphonium (TPP) mitochondria-targeting fragment as part of the molecular design (Scheme 4(a)).<sup>31</sup> While localized CO release was realized, as evidenced by the release of a fluorescent byproduct, no examination of the effects of CO delivery on mitochondrial bioenergetics were reported. During the same time period our group was pursuing the preparation of **12** (Scheme 4), a triphenylphosphonium-tailed derivative of **1**.<sup>4</sup> Compound **12** retains all of the photophysical and CO release reactivity features of **1** while also exhibiting good cellular uptake and mitochondrial localization as indicated by confocal co-localization studies (Figure 10(b) and (c); Pearson's co-localization coefficient with Mitotracker Red  $0.707 \pm 0.014$  for 29 examined cells). MTT studies of **12** in HUVECs and A549 cells revealed significant cytotoxicity, with mean  $\text{IC}_{50}$  values of  $1.51 \pm 1.4 \mu\text{M}$  and  $14.1 \pm 2.7 \mu\text{M}$ , respectively. Notably, visible light-induced CO release from **12** does not affect the toxicity of **12** in HUVECs ( $3.78 \pm 1.5 \mu\text{M}$ ) but does increase the toxicity in A549s ( $\text{IC}_{50}$   $4.6 \pm 3.6 \mu\text{M}$ ). Similar to other CO-release depside products described herein, **13** does not exhibit any cytotoxicity up to 100  $\mu\text{M}$ .

To gain insight into the effects of CO on mitochondrial function, we examined the influence of visible light-induced CO release from cytosolic **1** and mitochondria-localized **12** (0.1–10  $\mu\text{M}$ ) on mitochondrial bioenergetics in A549 cells using an Extracellular Flux Analyzer

(Agilent Seahorse XF).<sup>4</sup> The results were compared to those produced using (a) non-illuminated **1** and **12**, (b) the CO release products **2** and **13**, or c) a TPP tail model compound. These investigations revealed that under CO release conditions at 10  $\mu$ M both **1** and **12** produced similar effects, decreasing ATP production, maximal respiration, and the cell reserve capacity. This concentration is notably more than two-fold lower than that reported for metal carbonyl CORMs that are needed to produce similar biological effects. These combined results indicate that intracellular CO release from **1** and mitochondrial-targeted **12** produces more potent biological effects than the Ru(II)-containing CORM-2 and CORM-3. We hypothesize that this relates to the ability of the flavonol CORMs to deliver a localized intracellular concentration of CO whereas CORM-2 and CORM-3 likely release CO extracellularly.

### Protein Delivery of a Quinolone PhotoCORM

Targeted delivery of photoCORMs to cancer cells offers a new approach toward treating tumors using CO. Albumins are known to accumulate and be catabolized by tumors and have been used to deliver drugs to tumor sites.<sup>50</sup> In the CORM field, Bernardes, et al. enhanced CO accumulation at a colon carcinoma tumor site in mice using a protein-bound form of CORM-2.<sup>67</sup> The same complex provides significant downregulation of inflammatory markers such as cytokines interleukin (IL)-6, IL-10, and TNF- $\alpha$  in HeLa and Caco-2 cells.

A metal-free photoCORM based on a quinolone motif (**3**, Figure 11) binds tightly to BSA ( $K_a \sim 3.0 \times 10^6 \text{ M}^{-1}$ ).<sup>2</sup> Visible light-induced CO release from this BSA-quinolone conjugate produces potent anti-cancer effects in A549 cells at a concentration as low as 24  $\mu$ M. The protein:**3** conjugate also produces an unprecedented suppression of TNF- $\alpha$  production in LPS-challenged murine macrophages (RAW 264.7 cells) at 80 nM. Notably, a prodrug form of **3**, the diketone **14** (Figure 11), is reduced by cellular thiols, which suggests possible activation in the reducing environment of cancer cells. Overall, the quinolone framework offers a second novel framework on which to build triggerable, trackable, and targetable CO-releasing compounds.

## V. Perspective and Outlook

Interest in CO as a bioactive molecule and as a potential therapeutic has grown rapidly over the past decade. A persistent challenge in the field has been the safe delivery of controlled amounts of CO so as to limit toxicity. Since the mid-2000s, metal carbonyl complexes, especially the Ru(II)-containing CORM-2 and CORM-3, have been the most commonly employed CO delivery agents for many biological studies directed at probing the effects of this diatomic molecule. While metal-dependent reactivity other than CO release for these complexes initially received little attention, recent reports have made clear that the redox reactivity of Ru(II) could be producing some of the observed biological effects.<sup>20–22</sup> This issue provides strong impetus for the development of metal-free CORMs for which the CO release byproducts can be conclusively identified and evaluated independently in terms of their biological properties.

To date only a few types of organic molecules have been developed for CO delivery in biological environments, with two specific frameworks being more significantly advanced. Wang and co-workers are developing norborn-2-en-7-one derivatives formed via alkyne/Diels-Alder reactivity for spontaneous, systemic CO release and potential therapeutic applications.<sup>29</sup> Our work outlined herein has been directed primarily at developing extended flavonols and quinolones as triggered CO-releasing molecular tools, photoCORMs that enable significant spatial/temporal control of CO release. A key feature of these photoCORMs is that they do not exhibit CO leakage, thus allowing for localized CO release. The successful demonstrations of the uses of these compounds for CO delivery in cells and animals outlined herein sets the stage for their further biological applications. Notably, unlike many CORMs, **1** and **3** have well-defined CO release organic products that are nontoxic.

In terms of further CORM development, photoCORMs with enhanced trackability in cellular environments are needed to elucidate the local effects of CO release. A challenge in using **1** and **3** as trackable CORMs can be the moderate intensity and rapid bleaching (due to CO release) of their fluorescent emission signals under confocal microscopy conditions in air. In fact, we have found that **1** is most easily visualized in cells following bioanalyte-triggered deprotection of a 3-OR functionalized scaffold (e.g., R = thiol sensor **4**).<sup>3</sup> This improved visualization may relate to better cellular uptake of the protected compounds due to enhanced hydrophobicity. We note that mitochondrial localization of **12** also results in enhanced emission intensity due to targeted accumulation. An immediate goal of our research is the development of analogs of **1** with enhanced fluorescent emission properties to enable trackability at lower concentrations under confocal microscopy conditions.

The ability to target triggerable CORMs (e.g., photoCORMs) to specific subcellular locations is also critical for understanding the effects of exogenous CO delivery versus endogenous CO generation from HO-1. Under normal conditions, HO-1 is localized in the endoplasmic reticulum with exposure to the cytosol. Under stress conditions, HO-1 also is found in mitochondria, calveolae, and nucleus.<sup>65</sup> To date, there is no known CORM that has been shown to mimic the localization of HO-1.

Overall, extended flavonol and quinolone-based photoCORM frameworks offer a rich environment for the development of a broad array of biologically active CO-releasing compounds. A key feature that makes this class of molecules potentially very useful is the likelihood that quantitative visible light-induced CO release reactivity from the pyrone ring will be retained while the aromatic rings are functionalized. We are continuing to explore this rich landscape by generating molecular tools to advance understanding of the role of CO in human health and disease.

## Acknowledgements:

We thank the NIH (R15GM124596 to L.M.B. and A.D.B.), the Utah Agricultural Experiment Station (projects UTA-1178 and UTA-1456 to A.D.B.), the American Heart Association (grant 18PRE34030099 to T.S.), and the USU Office of Research (PDRF Fellowship to T.S.) for financial support.

## Biosketches

**Livia S. Lazarus (formerly Tatiana Soboleva)** received her B.S. in Biochemistry from Minnesota State University, Mankato in 2016. She is currently a Presidential Doctoral Research Fellow and American Heart Association Predoctoral Fellow at Utah State University working on her Ph.D. in organic chemistry under the direction of Professor Lisa M. Berreau. Livia is exploring the chemical properties and biological effects of visible light-induced CO-releasing molecules based on a 3-hydroxyflavone motif.

**Abby D. Benninghoff** received her B.S. in Biology and Biochemistry from the University of Tennessee, Knoxville and her Ph.D. in Marine Science from the University of Texas at Austin. She completed her post-doctoral training in Toxicology at Oregon State University. Dr. Benninghoff is currently an Associate Professor of Toxicology at Utah State University and serves as the Associate Dean for Research and Graduate Student Services for the College of Agriculture and Applied Sciences. Her multidisciplinary research program leverages expertise in toxicology, cancer and nutrient-gene interactions to investigate the role of basal diet and dietary bioactives on gut inflammation and cancer prevention.

**Lisa M. Berreau** received her B.S. in Chemistry from Minnesota State University, Mankato and her Ph.D. in Inorganic Chemistry from Iowa State University, Ames. She was an NIH Postdoctoral Fellow at the University of Minnesota. She is currently a Professor of Chemistry and serves as the Vice President for Research at Utah State University. Her research program focuses on elucidating structure/reactivity relationships in reactions involving O<sub>2</sub> activation and applying the insight gained to the development of novel compounds, including flavonol-based CO-releasing molecules.

## References

1. Popova M; Soboleva T; Arif AM; Berreau LM Properties of a Flavonol-based PhotoCORM in Aqueous Buffered Solutions: Influence of Metal Ions, Surfactants and Proteins on Visible Light-Induced CO Release. *RSC. Adv* 2017, 7, 21997–22007. DOI: 10.1039/C7RA02653F
2. Popova M; Soboleva T; Ayad S; Benninghoff AD; Berreau LM Visible Light-Activated Quinolone Carbon-Monoxide-Releasing Molecule: Prodrug and Albumin-Assisted Delivery Enables Anticancer and Potent Anti-inflammatory Effects. *J. Am. Chem. Soc* 2018, 140, 9721–9729. DOI: 10.1021/jacs.8b06011 [PubMed: 29983046]
3. Soboleva T; Esquer HJ; Benninghoff AD; Berreau LM Sense and Release: A Thiol-responsive Flavonol-Based Photonically Driven Carbon Monoxide-Releasing Molecule that Operates via a Multiple-input AND Logic Gate. *J. Am. Chem. Soc* 2017, 139, 9435–9438. DOI: 10.1021/jacs.7b04077 [PubMed: 28677975]
4. Soboleva T; Esquer HJ; Anderson SN; Berreau LM Benninghoff AD Mitochondrial-localized versus Cytosolic Intracellular CO-Releasing Organic PhotoCORMs: Evaluation of CO Effects Using Bioenergetics. *ACS Chem. Biol* 2018, 13, 2220–2228. DOI: 10.1021/acscchembio.8b00387 [PubMed: 29932318]
5. Wu L; Wang R Carbon Monoxide: Endogenous Production, Physiological Functions, and Pharmacological Applications. *Pharmacol Rev* 2005, 57, 585–630. DOI: 10.1124/pr.57.4.3 [PubMed: 16382109]
6. Peers C; Boyle JP; Scragg JL; Dallas ML; Al-Owais MM; Hettiarachichi NT; Elies J; Johnson E; Gamper N; Steele DS Diverse Mechanisms Underlying the Regulation of Ion Channels by Carbon Monoxide. *Br. J. Pharmacol* 2015, 172, 1546–1556. DOI: 10.1111/bph.12760 [PubMed: 24818840]

7. Walewska A; Szewczyk A; Koprowski P Gas Signaling Molecules and Mitochondrial Potassium Channels. *Int. J. Mol. Sci* 2018, 19, 3227 DOI: 10.3390/ijms19103227
8. Motterlini R; Foresti R Biological Signaling by Carbon Monoxide and Carbon Monoxide Releasing Molecules. *Am. J. Physiol. Cell Physiol* 2017, 312, C302–C313. DOI: 10.1152/ajpcell.00360.2016 [PubMed: 28077358]
9. Otterbein LE; Foresti R; Motterlini R Heme Oxygenase-1 and Carbon Monoxide in the Heart: The Balancing Act Between Danger Signaling and Pro-survival. *Circ. Res* 2020, 118, 1940–1959. DOI: <http://10.1161/CIRCRESAHA.116.306588>
10. Ryter S Heme Oxygenase-1/Carbon Monoxide as Modulators of Autophagy and Inflammation. *Arch. Biochem. Biophys* 2019, 678, 108186 DOI: 10.1016/j.abb.2019.108186 [PubMed: 31704095]
11. Goebel U; Wollborn J Carbon Monoxide in Intensive Care Medicine - Time to Start the Therapeutic Application?! *Intensive Care Med. Exp* 2020, 8:2 DOI: 10.1186/s40635-020-0292-8
12. Zhao Y; Yu W; Cao J; Gao H Harnessing Carbon Monoxide-Releasing Platforms for Cancer Therapy. *Biomaterials* 2020, 255, 120193 DOI: 10.1016/j.biomaterials.2020.120193 [PubMed: 32569866]
13. Motterlini R; Otterbein LE The Therapeutic Potential of Carbon Monoxide. *Nat. Rev Drug Discov* 2010, 9, 728–743. DOI: 10.1038/nrd3228 [PubMed: 20811383]
14. Hopper CP; Meinel L; Steiger C; Otterbein LE Where is the Clinical Breakthrough of Heme Oxygenase-1/Carbon Monoxide Therapeutics? *Curr. Pharm. Des* 2018, 24, 2264–2282. DOI: 10.2174/1381612824666180723161811 [PubMed: 30039755]
15. Mann BE CO-Releasing Molecules: A Personal View. *Organometallics* 2012, 31, 5728–5735. DOI: 10.1021/om300364a
16. Motterlini R; Clark JE; Foresti R; Sarathchandra P; Mann BE; Green CJ Carbon Monoxide-Releasing Molecules Characterization of Biochemical and Vascular Activities. *Circ Res* 2002, 90, E17–24. DOI: 10.1161/hh0202.104530 [PubMed: 11834719]
17. Foresti R; Hammad J; Clark JE; Johnson TR; Mann BE; Friebe A; Green CJ; Motterlini R Vasoactive Properties of CORM-3, A Novel Water-soluble Carbon Monoxide-Releasing Molecule. *Br. J. Pharmacol* 2004, 14, 453–460. DOI: 10.1038/sj.bjp.0705825
18. Crook SH; Mann BE; Meijer AJHM; Adams H; Sawle P; Scapens D; Motterlini RM [Mn(CO)<sub>4</sub>{S<sub>2</sub>CNMe(CH<sub>2</sub>CO<sub>2</sub>H)}], a New Water-Soluble CO-Releasing Molecule. *Dalton Trans* 2011, 40, 4230–4235. DOI: 10.1039/c1dt10125k [PubMed: 21403944]
19. Santos-Silva T; Mukhopadhyay A; Seixas JD; Bernardes GJL; Romão CC; Romão MJ CORM-3 Reactivity Toward Proteins: The Crystal Structure of a Ru(II) Dicarboxyl-lysozyme Complex. *J. Am. Chem. Soc* 2011, 133, 1192–1195. DOI: 10.1021/ja108820s [PubMed: 21204537]
20. Yuan Z; Yang X; de La Cruz LK; Wang B Nitro-reduction Based Fluorescent Probes for Carbon Monoxide Require Reactivity Involved a Ruthenium Carbonyl Moiety. *Chem. Commun* 2020, 56, 2190–2193.
21. Southam HM; Smith TW; Lyon RL; Liao C; Trevitt CR; Middlemiss LA; Cox FL; Chapman JA; El-Khamisy SF; Hippler M; Williamson MP; Henderson PJF; Poole RK A Thiol-reactive Ru(II) Ion, Not CO Release, Underlies the Potent Antimicrobial and Cytotoxic Properties of CO-releasing Molecule-3. *Redox Biol* 2018, 18, 114–123. DOI: 10.1016/j.redox.2018.06.008 [PubMed: 30007887]
22. Stucki D; Krahl H; Walter M; Steinhausen J; Hommel K; Brenneisen P; Stahl W Effects of Frequently Applied Carbon Monoxide Releasing Molecules (CORMs) in Typical CO-sensitive Model Systems – A Comparative In Vitro Study. *Arch. Biochem. Biophys* 2020, 687, 108383 DOI: 10.1016/j.abb.2020.108383 [PubMed: 32335048]
23. Kottelat E; Zobi F Visible Light-Activated PhotoCORMs. *Inorganics* 2017, 5, 24 DOI: 10.3390/inorganics5020024
24. Sitnikov NS; Li Y; Zhang D; Yard B; Schmalz H–G Design, Synthesis, and Functional Evaluation of CO-releasing Molecules Triggered by Penicillin G Amidase as a Model Protease. *Angew. Chem. Int. Ed. Engl* 2015, 54, 12314–12318. DOI: 10.1002/anie.201502445 [PubMed: 26037072]

25. Kunz PC; Meyer H; Barthel J; Sollazzo S; Schmidt AM; Janiak C Metal Carbonyls Supported on Iron Oxide Nanoparticles to Trigger the CO-Gasotransmitter Release by Magnetic Heating. *Chem. Commun* 2013, 49, 4896–4898. DOI: 10.1039/C3CC41411F
26. Soboleva T; Berreau LM Tracking CO Release in Cells via the Luminescence of Donor Molecules and/or Their By-products. *Isr. J. Chem* 2019, 59, 339–350. DOI: 10.1002/ijch.201800172 [PubMed: 31516159]
27. Faizan M; Muhammed N; Niazi KUK; Hu Y; Wang Y; Wu Y; Sun H; Liu R; Dong W; Zhang W; Gao Z CO-Releasing Materials: An Emphasis on Therapeutic Implications, as Release and Subsequent Cytotoxicity are the Part of Therapy. *Materials* 2019, 12, 1643 DOI: 10.3390/ma12101643
28. Motterlini R; Sawle P; Hammad J; Bains S; Alberto R; Foresti R; Green CJ CORM-A1: A New Pharmacologically Active Carbon Monoxide-Releasing Molecule. *FASEB J* 2005, 19, 284–286. DOI: 10.1096/fj.04-2169fje [PubMed: 15556971]
29. Ji X; Wang B Strategies Toward Organic Carbon Monoxide Prodrugs. *Acc. Chem. Res* 2018, 51, 1377–1385. DOI: 10.1021/acs.accounts.8b00019 [PubMed: 29762011]
30. Yang X; de Caestecker M; Otterbein LE; Wang B Carbon Monoxide: An Emerging Therapy for Acute Kidney Injury. *Med. Res. Rev* 2019, 1–31. DOI: 10.1002/med.21650
31. Zheng Y; Ji X; Yu B; Ji K; Gallo D; Csizmadia E; Zhu M; Choudhary MR; De la Cruz LKC; Chittavong V; Pan Z; Yun Z; Otterbein LE; Wang B Enrichment-Triggered Prodrug Activation Demonstrated Through Mitochondria-Targeted Delivery of Doxorubicin and Carbon Monoxide. *Nature Chem* 2018, 10, 787–794. DOI: 10.1038/s41557-018-0055-2 [PubMed: 29760413]
32. Ji X; Pan Z; Li C; Kang T; De La Cruz LKC; Yang L; Yuan Z; Ke B; Wang B Esterase-sensitive and pH-Controlled Carbon Monoxide Prodrugs for Treating Systemic Inflammation. *J. Med. Chem* 2019, 62, 3163–3168. DOI: 10.1021/acs.jmedchem.9b00073 [PubMed: 30816714]
33. Peng P; Wang C; Shi Z; Johns VK; Ma L; Oyer J; Copik A; Igarashi R; Liao Y Visible-light Activatable Organic CO-Releasing Molecules (PhotoCORMs) that Simultaneously Generate Fluorophores. *Org. Biomol. Chem* 2013, 11, 6671–6674. DOI: 10.1039/C3OB41385C [PubMed: 23943038]
34. Antony LAP; Slanina T; Šebej P; Šolomek T; Klán P Fluorescein Analogue Xanthene-9-Carboxylic Acid: A Transition-Metal-Free CO Releasing Molecule Activated by Green Light. *Org. Lett* 2013, 15, 4552–4555. DOI: 10.1021/ol4021089 [PubMed: 23957602]
35. Palao E; Slanina T; Muchová L; Šolomek T; Vitek L; Klán P Transition-Metal-Free CO-releasing BODIPY Derivatives Activatable by Visible to NIR Light as Promising Bioactive Molecules. *J. Am. Chem. Soc* 2016, 138, 126–133. DOI: 10.1021/jacs.5b10800 [PubMed: 26697725]
36. De La Cruz LKC; Benoit SL; Pan Z; Yu B; Maier RJ; Ji X; Wang B Click, Release, and Fluoresce: A Chemical Strategy for a Cascade Prodrug System for Co-delivery of Carbon Monoxide, a Drug Payload, and a Fluorescent Reporter. *Org. Lett* 2018, 20, 897–900. DOI: 10.1021/acs.orglett.7b03348 [PubMed: 29380605]
37. Kautz AC; Kunz PC; Janiak C CO-Releasing Molecule (CORM) Conjugate Systems. *Dalton Trans* 2016, 45, 18045–18063. DOI: 10.1039/C6DT03515A [PubMed: 27808304]
38. Kawahara B; Gao L; Cohn W; Whitelegge JP; Sen S; Janzen C; Mashchak PK Diminished Viability of Human Ovarian Cancer Cells by Antigen-Specific Delivery of Carbon Monoxide with a Family of Photoactivatable Antibody-PhotoCORM Conjugates. *Chem. Sci* 2020, 11, 467–473. DOI: 10.1039/C9SC03166A
39. Jin Z; Wen Y; Xiong L; Yang T; Zhao P; Tan L; Wang T; Qian Z; Su B -L.; He, Q. Intratumoral H<sub>2</sub>O<sub>2</sub>-triggered Release of CO from a Metal Carbonyl-based Nanomedicine for Efficient CO Release. *Chem. Commun* 2017, 53, 5557–5560. DOI: 10.1039/C7CC01576C
40. Yan H; Du J; Zhu S; Nie G; Zhang H; Gu Z; Zhao Y Emerging Delivery Strategies of Carbon Monoxide for Therapeutic Applications: From CO Gas to CO Releasing Nanomaterials. *Small* 2019, 15, 1904382 DOI: 10.1002/sml.201904382
41. Patel RV; Mistry BM; Shinde SK; Syed R; Singh V; Shin HS Therapeutic Potential of Quercetin as a Cardiovascular Agent. *Eur. J. Med. Chem* 2018, 155, 889–904. DOI: 10.1016/j.ejmech.2018.06.053 [PubMed: 29966915]

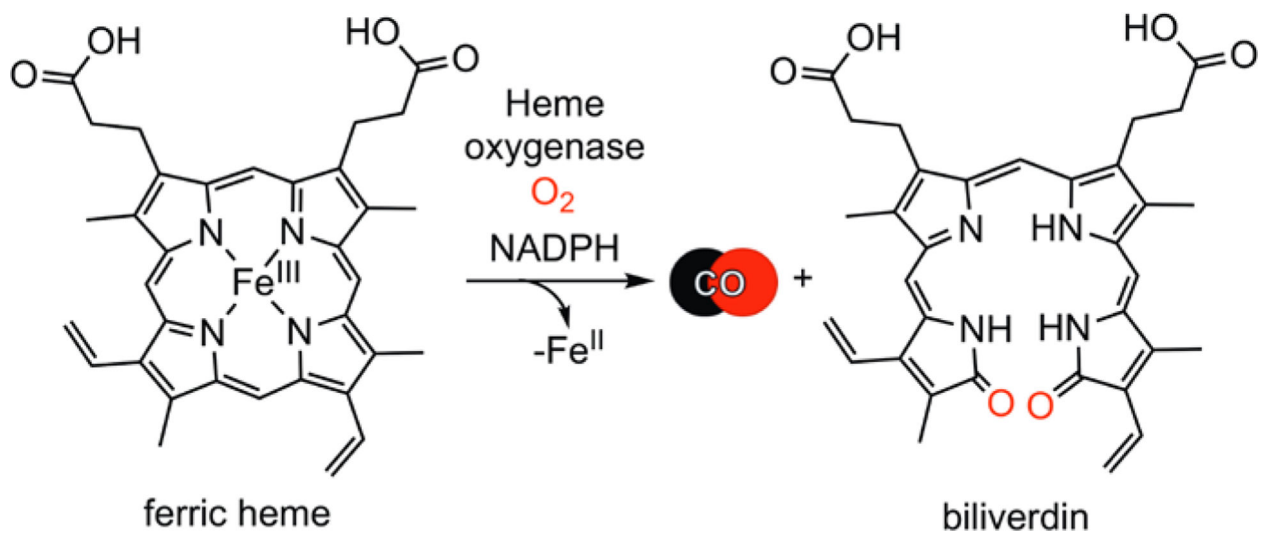
42. Rauf A; Imran M; Khan IA; Ur-Rehman M; Gilani SA; Mehmood Z; Mubarak MS Anticancer Potential of Quercetin: A Comprehensive Review. *Phytother. Res* 2018, 32, 2109–2130. DOI: 10.1002/ptr.6155 [PubMed: 30039547]
43. Fetzner S Ring-cleaving Dioxygenases with a Cupin Fold. *Appl. Environ. Microbiol* 2012, 78, 2505–2514. DOI: 10.1128/AEM.07651-11 [PubMed: 22287012]
44. Soboleva T; Berreau LM 3-Hydroxyflavones and 3-Hydroxy-4-oxoquinolines as Carbon Monoxide-Releasing Molecules. *Molecules* 2019, 24, 1252 DOI: 10.3390/molecules24071252
45. Anderson SN; Richards JM; Esquer HJ; Benninghoff AD; Arif AM; Berreau LM A Structurally-tunable 3-Hydroxyflavone Motif for Visible Light-Induced Carbon Monoxide-Releasing Molecules (CORMs). *ChemistryOpen* 2015, 4, 590–594. DOI: 10.1002/open.201500167 [PubMed: 26491637]
46. Li Y; Shu Y; Liang M; Xie X; Jiao X; Wang X; Tang B A Two-Photon H<sub>2</sub>O<sub>2</sub>-Activated CO Photoreleaser. *Angew. Chem. Int. Ed* 2018, 57, 12415–12419. DOI: 10.1002/anie.201805806
47. Soboleva T; Simons CR; Arcidiacono A; Benninghoff AD; Berreau LM Extracellular vs Intracellular Delivery of CO: Does it Matter for a Stable, Diffusible Gasotransmitter? *J. Med. Chem* 2019, 62, 9990–9995. DOI: 10.1021/acs.jmedchem.9b01254 [PubMed: 31577143]
48. Russo M; Štacko P; Nachtigallová D; Klán P Mechanisms of Orthogonal Photodecarbonylation Reactions of 3-Hydroxyflavone-Based Acid-base Forms. *J. Org. Chem* 2020, 85, 3527–3537. DOI: 10.1021/acs.joc.9b03248
49. Bilokin MD; Shvadchak VV; Yushchenko DA; Klymchenko AS; Duportail G; Mely Y; Pivovarenko VG 3-Hydroxybenzo[g]quinolones: Dyes with Red-Shifted Absorption and Highly Resolved Dual Emission. *Tetrahedron Lett* 2009, 50, 4714–4719. DOI: 10.1016/j.tetlet.2009.06.024
50. Sleep D Albumin and its Application in Drug Delivery. *Expert Opin. Drug Deliv* 2015, 12, 793–812. DOI: 10.1517/17425247.2015.993313 [PubMed: 25518870]
51. Erbas-Cakmak S; Kolemen S; Sedgwick AC; Gunnlaugsson T; James TD; Yoon J; Akkaya EU Molecular Logic Gates: The Past, Present and Future. *Chem. Soc. Rev* 2018, 47, 2228–2248. DOI: 10.1039/C7CS00491E [PubMed: 29493684]
52. Andréasson J; Pischel U Molecules with a Sense of Logic: A Progress Report. *Chem. Soc. Rev* 2015, 44, 1053–1069. DOI: 10.1039/C4CS00342J [PubMed: 25520053]
53. Reddy U; Axthelm J; Hoffmann P; Taye N; Gläser S; Görls H; Hopkins SL; Plass W; Neugebauer U; Bonnet S; Schiller A Co-Registered Molecular Logic Gate with a CO-releasing Molecule Triggered by Light and Peroxide. *J. Am. Chem. Soc* 2017, 139, 4991–4994. DOI: 10.1021/jacs.7b00867 [PubMed: 28345936]
54. Yang X; Guo Y; Strongin RM Conjugate Addition/Cyclization Sequence Enables Selective and Simultaneous Fluorescence Detection of Cysteine and Homocysteine. *Angew. Chem. Int. Ed* 2011, 50, 10690–10693. DOI: 10.1002/anie.201103759
55. Dai J; Ma C; Zhang P; Fu Y; Shen B Recent Progress in the Development of Fluorescent Probes for Detection of Biothiols. *Dyes Pigm* 2020, 177, 108321 DOI: 10.1016/j.dyepig.2020.108321
56. McKeown SR Defining Normoxia, Physoxia and Hypoxia in Tumours -Implications for Treatment Response. *Br J. Radiol* 2014, 87, 20130676 DOI: 10.1259/bjr.20130676 [PubMed: 24588669]
57. Xie Z-Z; Liu Y; Bian J-S Hydrogen Sulfide and Cellular Redox Homeostasis. *Oxid. Med. Cell. Longev* 2016, 2016, 6043038 DOI: 10.1155/2016/6043038 [PubMed: 26881033]
58. Kabil O; Yadav V; Banerjee R Heme-dependent Metabolite Switching Regulates H<sub>2</sub>S Synthesis in Response to Endoplasmic Reticulum (ER) Stress. *J. Biol. Chem* 2016, 291, 16418–16423. DOI: 10.1074/jbc.C116.742213 [PubMed: 27365395]
59. Peng Y-J; Zhang X; Gridina A; Chupikova I; McCormick DL; Thomas RJ; Scammell TE; Kim G; Vasavda C; Nanduri J; Kumar GK; Semeza GL; Snyder SH; Prabhakar NR Complementary Roles of Gasotransmitters CO and H<sub>2</sub>S in Sleep Apnea. *Proc. Natl. Acad. Sci. USA* 2017, 114, 1413–1418. DOI: 10.1073/pnas.162717114 [PubMed: 28115703]
60. Soboleva T; Benninghoff AD; Berreau LM An H<sub>2</sub>S-sensing/CO-releasing Flavonol that Operates via Logic Gates. *ChemPlusChem* 2017, 82, 1408–1412. DOI: 10.1002/cplu.201700524 [PubMed: 30167353]

61. Lin VS; Chen W; Xian M; Chang CJ Chemical Probes for Molecular Imaging and Detection of Hydrogen Sulfide and Reactive Sulfur Species in Biological Systems. *Chem. Soc. Rev* 2015, 44, 4596–4618. DOI: 10.1039/C4CS00298A [PubMed: 25474627]
62. Wang R; Wang Z; Wu L Carbon Monoxide-induced Vasorelaxation and the Underlying Mechanisms. *Br. J. Pharmacol* 1997, 121, 927–934. DOI: 10.1038/sj.bjp.0701222 [PubMed: 9222549]
63. Popova M; Soboleva T; Benninghoff AD; Berreau LM CO Sense and Release Flavonols: Progress Toward the Development of an Analyte Replacement PhotoCORM for Use in Living Cells. *ACS Omega* 2020, 5, 10021–10033. DOI: 10.1021/acsomega.0c00409
64. Cheng J; Zheng B; Cheng S; Zhang G; Hu J Metal-free Carbon Monoxide-Releasing Micells Undergo Tandem Photochemical Reactions for Cutaneous Wound Healing. *Chem. Sci* 2020, 11, 4499–4507. DOI: 10.1039/D0SC00135J
65. Ryter SW; Alam J; Choi AMK Heme Oxygenase-1/Carbon Monoxide: From Basic Science to Therapeutic Applications. *Physiol. Rev* 2006, 86, 583–650. DOI: 10.1152/physrev.00011.2005
66. Cho Y-H; Kim N-H; Khan I; Yu JM; Jung HG; Kim HH; Jang JY; Kim HJ; Kim D-I; Kwak J-H; Kang SC; An BJ Anti-Inflammatory Potential of Quercetin-3-O- $\beta$ -D-(“2”-galloyl)-glucopyranoside and Quercetin Isolated from *Diospyros kaki* Calyx via Suppression of MAP Signaling Molecules in LPS-induced RAW 264.7 Macrophages. *J. Food Sci* 2016, 81, C2447–C2456. DOI: 10.1111/1750-3841.13497 [PubMed: 27648736]
67. Chaves-Ferreira M; Albuquerque IS; Matak-Vinkovic D; Coelho AC; Carvalho SM; Saraiva LM; Romão CC; Bernardes GJL Spontaneous CO Release from Ru<sup>II</sup>(CO)<sub>2</sub>-protein Complexes in Aqueous Solution, Cells, and Mice. *Angew. Chem. Int. Ed* 2015, 54, 1172–1175. DOI: 10.1002/anie.201409344

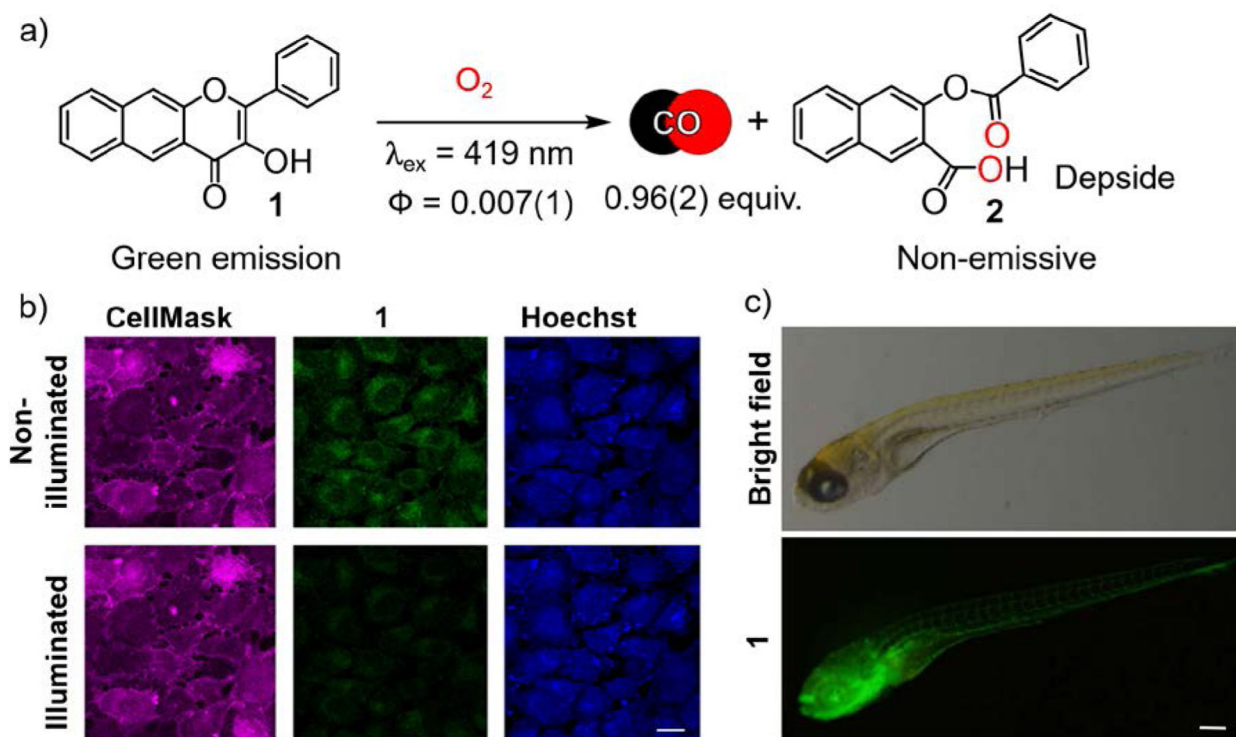
## Key References:

- Popova M; Soboleva T; Arif AM; Berreau LM Properties of a flavonol-based photoCORM in aqueous buffered solutions: Influence of metal ions, surfactants and proteins on visible light-induced CO release. *RSC Advances* 2017, 7, 21997–22007.<sup>1</sup> A fluorescence trackable extended flavonol is shown to: (1) exist in neutral or anionic form at pH = 7.4 depending on the buffer and the presence of surfactants; (2) weakly interact with bovine serum albumin; and (3) exhibit a quantum yield for CO release that depends on protonation level.
- Popova M; Soboleva T; Ayad S; Benninghoff AD; Berreau LM Visible-light-activated quinolone carbon-monoxide-releasing molecule: Prodrug and albumin-assisted delivery enables anticancer and potent anti-inflammatory effects. *J. Am. Chem. Soc* 2018, 140, 9721–9729. [PubMed: 29983046]<sup>2</sup> A quinolone photoCORM and its prodrug oxidized form offer new approaches for controlled CO delivery, with a quinolone:protein conjugate producing anti-cancer effects and significant anti-inflammatory outcomes at nanomolar concentrations.
- Soboleva T; Esquer HJ; Benninghoff AD; Berreau LM Sense and release: A thiol-responsive flavonol-based photonically driven carbon monoxide-releasing molecule that operates via a multiple-input AND logic gate. *J. Am. Chem. Soc* 2017, 139, 9435–9438. [PubMed: 28677975]<sup>3</sup> An extended flavonol derivative is shown to operate via AND logic gates by first sensing the cellular environment via detection of a cellular redox biomarker (thiols) followed by visible light-triggered CO release.
- Soboleva T; Esquer HJ; Anderson SN; Berreau LM; Benninghoff AD Mitochondrial-localized versus cytosolic intracellular CO-releasing organic photoCORMs: Evaluation of CO effects using bioenergetics. *ACS Chem. Biol* 2018, 13, 2220–2228. [PubMed: 29932318]<sup>4</sup> At a concentration of 10  $\mu$ M, mitochondrial-localized and cytosolic CO-releasing compounds produce similar outcomes in terms of decreasing ATP production, maximal respiration and the reserve capacity of A549 cells.



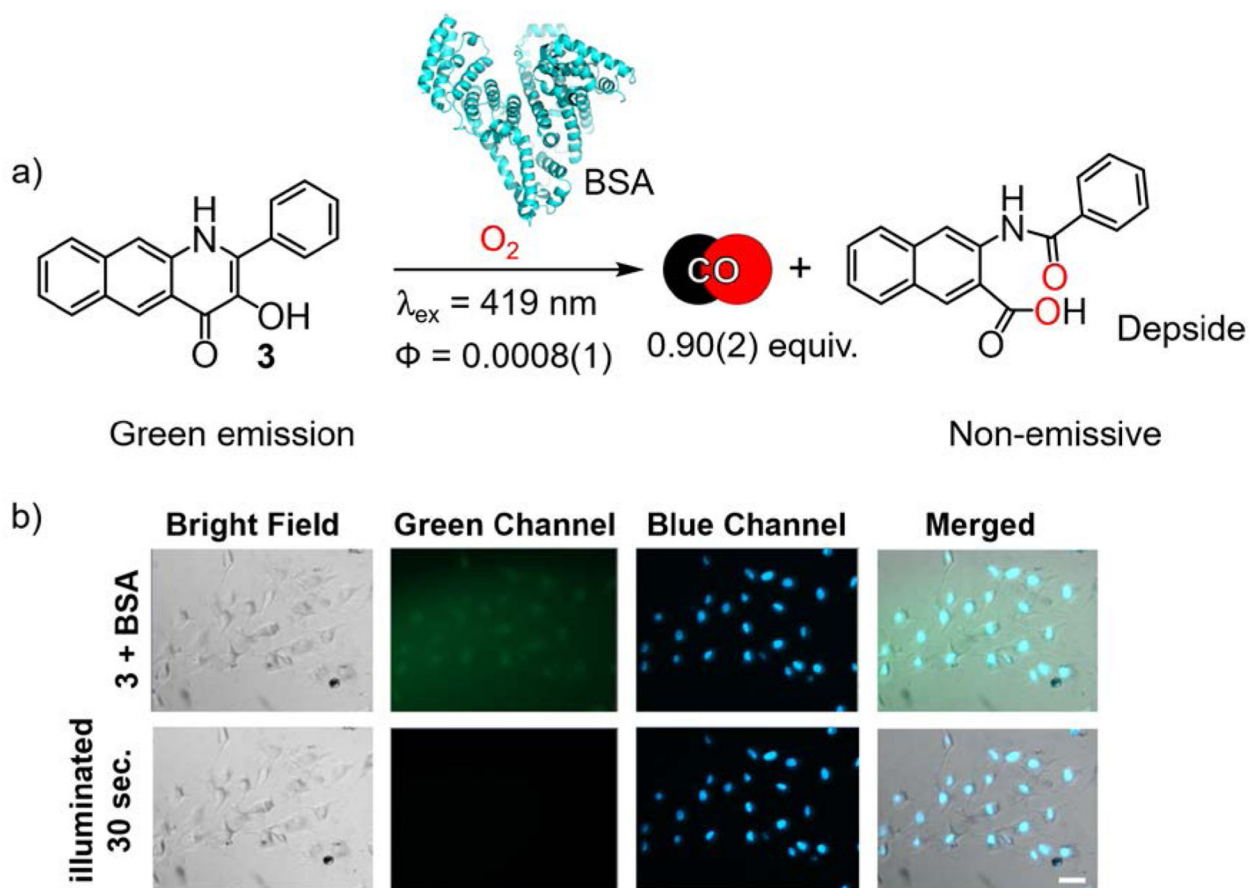


**Figure 1.**  
Catabolism of heme to produce CO and biliverdin.

**Figure 2.**

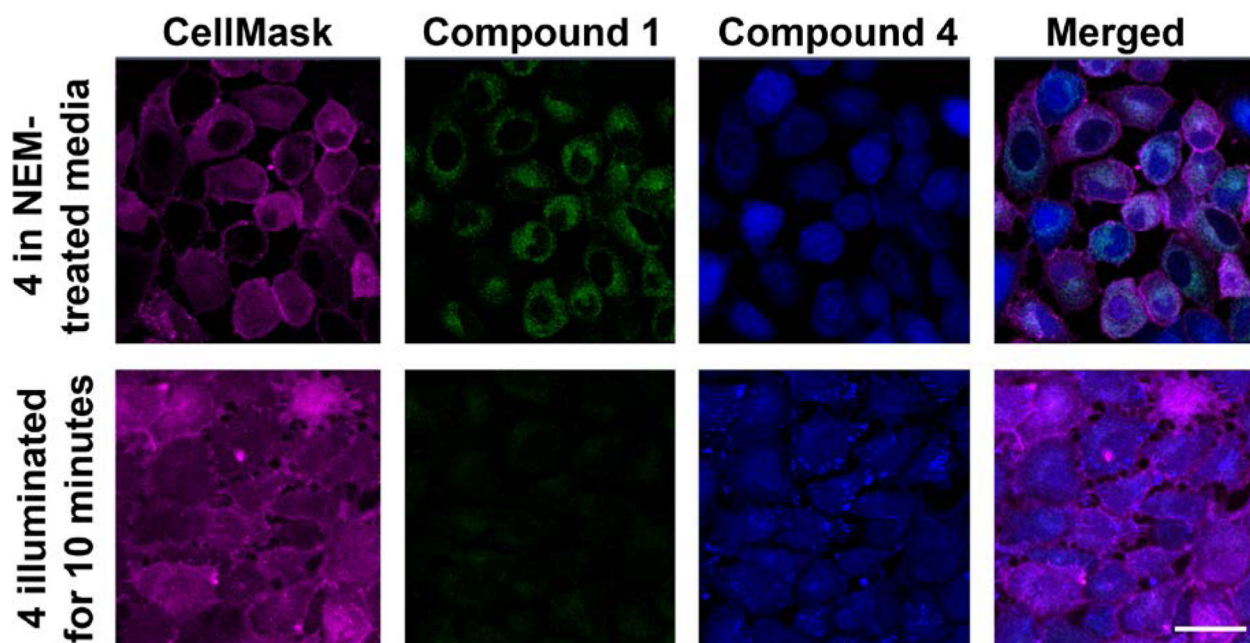
a) CO release reaction from **1**. b) A549 cells ( $10.00 \times 10^4$  cells/cm<sup>2</sup>) after 4 h of incubation with **1** ( $[1] = 50 \mu\text{M}$ ); Scale bar = 30  $\mu\text{m}$ . Adapted with permission from reference 3.

Copyright 2017 American Chemical Society. c) Fluorescent imaging of transgenic line of zebrafish, Tg (flila: EGFP) detecting **1**. Fluorescent images were acquired upon excitation with 488 nm wavelength and emission detection at  $\lambda_{\text{em}} = 500 - 550$  nm. Scale bar = 0.5 mm. Adapted with permission from reference 46. Copyright 2018 John Wiley and Sons.



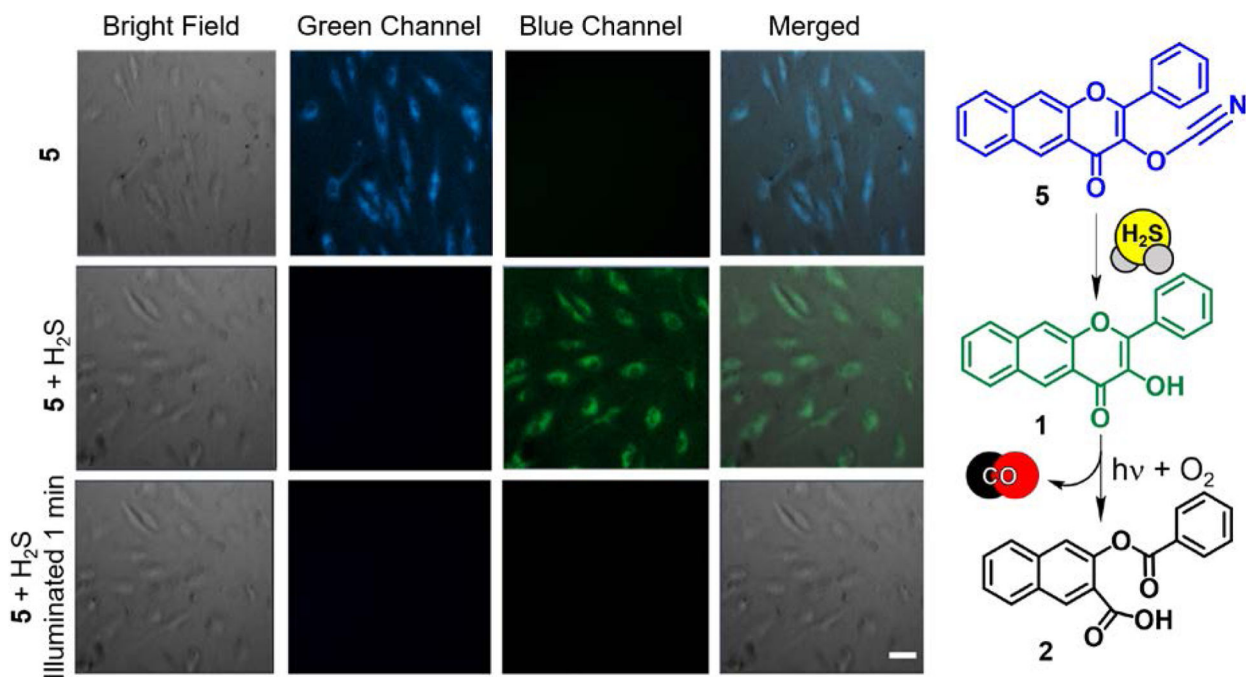
**Figure 3.**

a) CO release reaction from **3** in the presence of BSA. b) HUVECs pretreated with BSA and incubated for 4 h with **3** (50  $\mu\text{M}$ ). Scale bar = 50  $\mu\text{m}$ . Adapted with permission from reference 2. Copyright 2018 American Chemical Society.

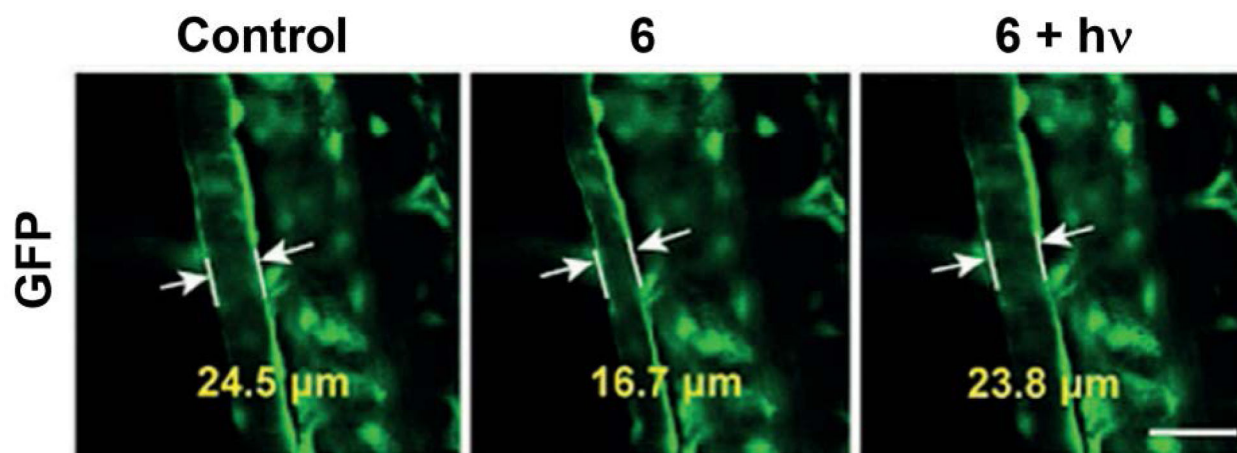


**Figure 4.**

Individual confocal images of A549 cells incubated with **4** (0.025 mM) for 1 h in NEM-treated media (line 1); and exposed to light ( $11.5 \text{ mW/cm}^2$  at 6% laser power) resulting in CO release from **1** and loss of emission (line 2). Adapted with permission from reference 3. Copyright 2017 American Chemical Society.

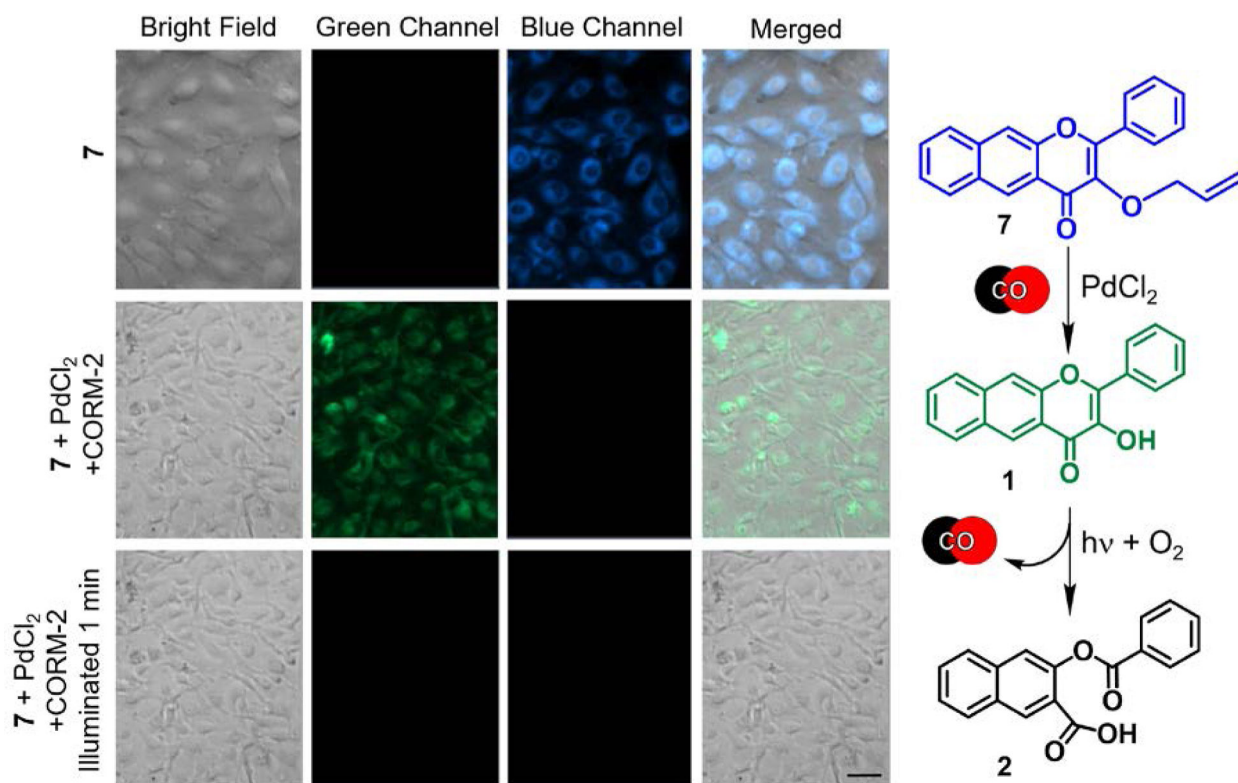


**Figure 5.** (left) Fluorescence microscopy studies of the reactivity of **5** in HUVECs. First row: **5** incubated for 24 hours ( $[\mathbf{5}] = 50 \mu\text{M}$ ). Second row: cells incubated with **5** following the addition of H<sub>2</sub>S (10  $\mu\text{M}$ ). Third row: Illumination of cells from second row (488 nm, 42620 lx) for 1 minute. Scale bar: 50  $\mu\text{m}$ . (right) Proposed H<sub>2</sub>S-sensing/CO-releasing reaction of **5** in cells. Adapted with permission from reference 60. Copyright 2017 John Wiley and Sons.

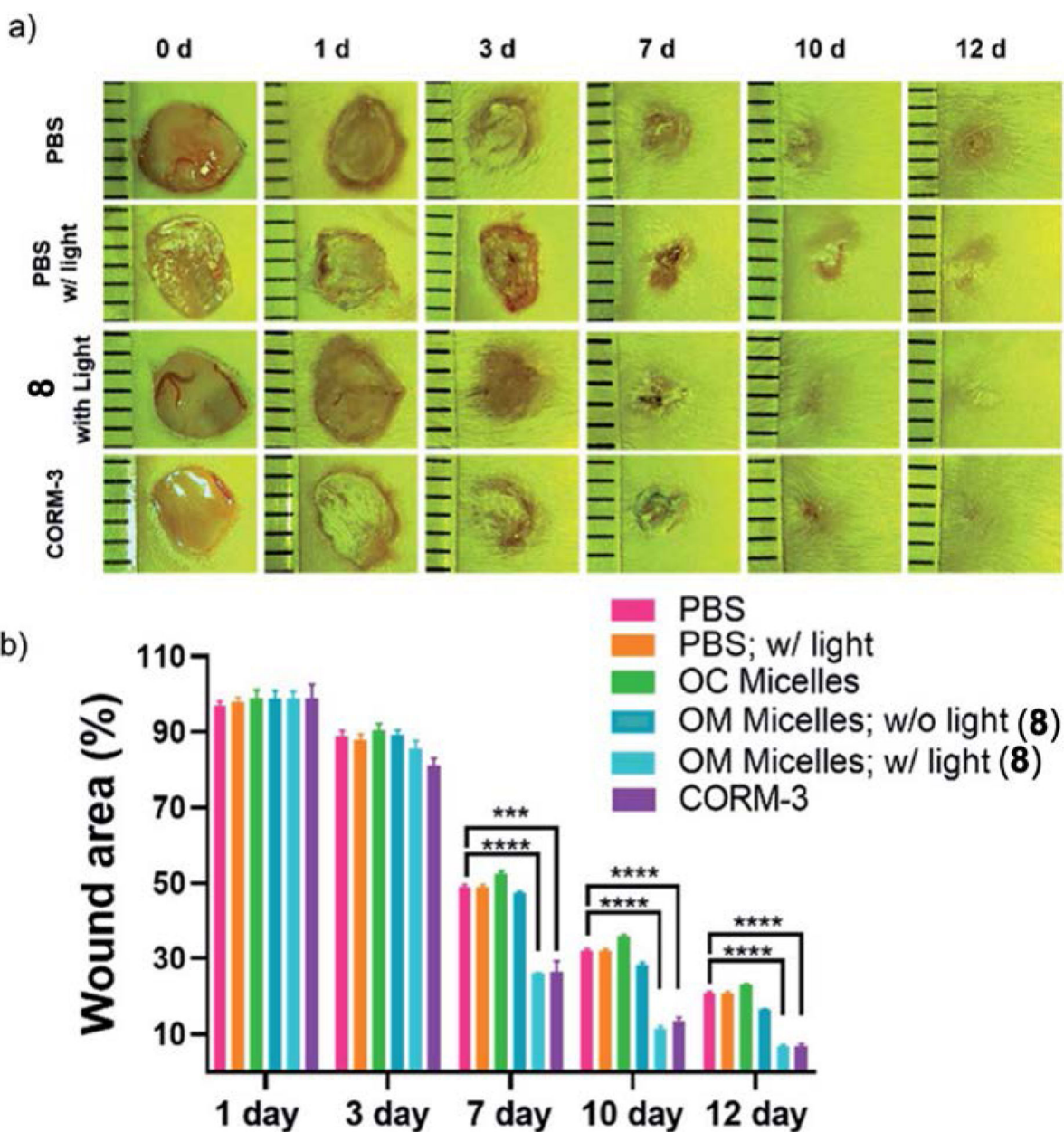


**Figure 6.**

The vasodilatation effect of CO in Tg zebrafish (Tg (filia: EGFP)) and angiotensin-II-induced  $H_2O_2$  fluctuation. (left) control. (middle) Tg zebrafish soaked with **6** ( $20 \mu M$ ) for 15 min and then exposed to angiotensin II (2 h). (right) Tg zebrafish from middle panel illuminated with 800 nm laser for 5 min. Scale bar:  $50 \mu m$ . Adapted with permission from reference 46. Copyright 2018 John Wiley and Sons.

**Figure 7.**

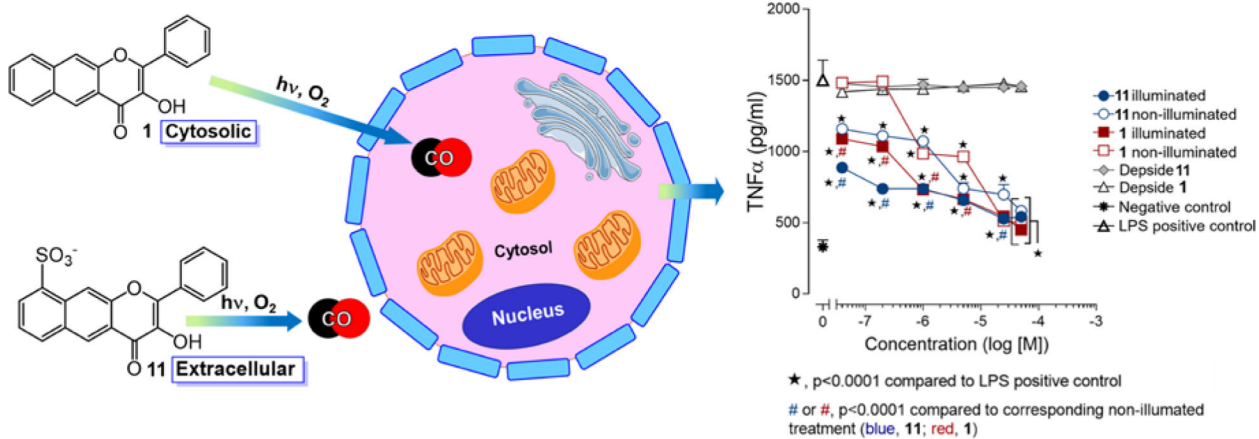
(left) Fluorescence microscopy studies of the reactivity of **7** in HUVECs. Top row: **7** incubated for 24 hours ( $[\mathbf{7}] = 50 \mu\text{M}$ ). Middle row: cells incubated with **7** following the addition of  $\text{PdCl}_2$  ( $100 \mu\text{M}$ ) and CORM-2 ( $500 \mu\text{M}$ ) as CO source. Bottom row: Illumination of cells from second row (488 nm, 42620 lx) for 1 minute. Scale bar: 40  $\mu\text{m}$ . (right) Proposed CO-sensing/CO-releasing reactions of **7** in cells. Adapted with permission from reference 63. Copyright 2020 American Chemical Society.



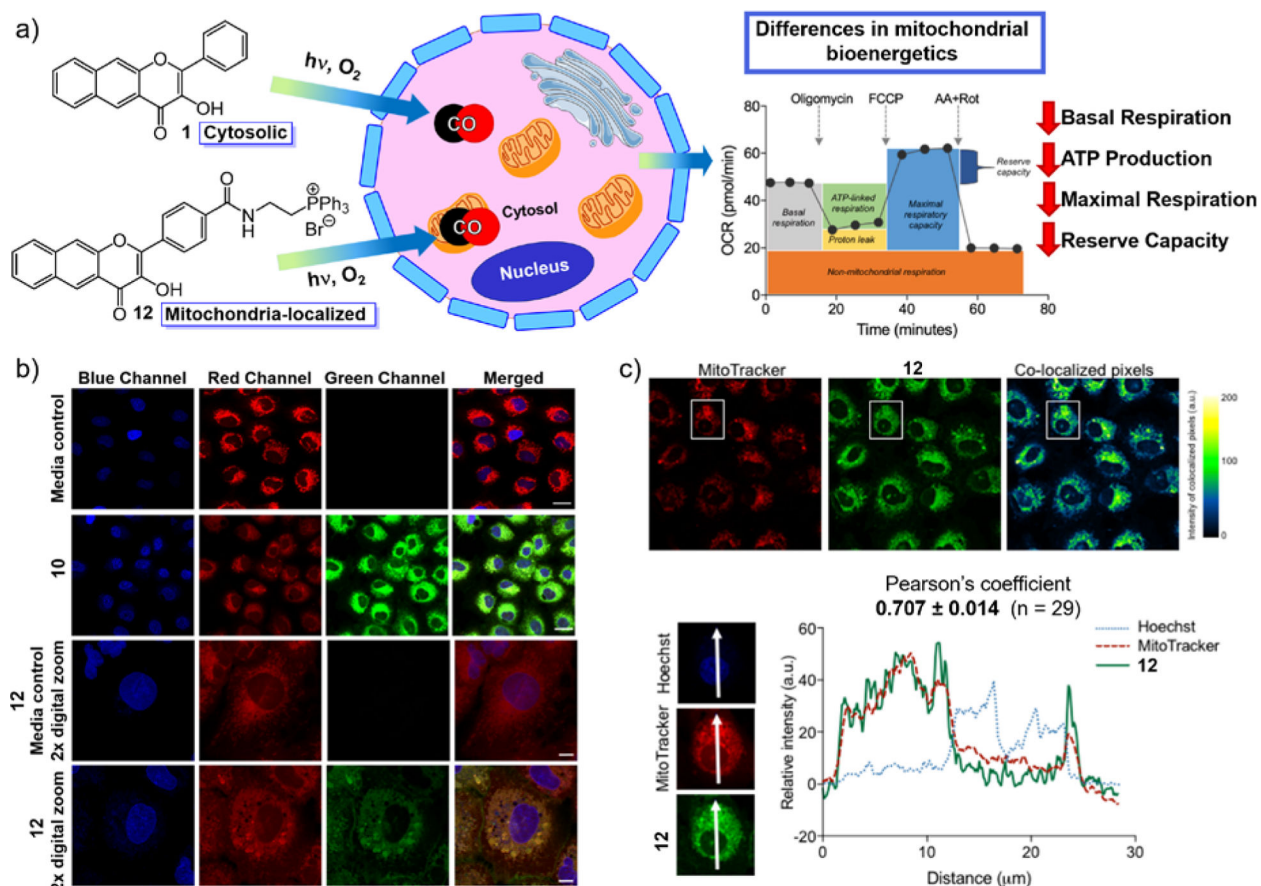
**Figure 8.**

(a) Representative images of cutaneous wounds treated with PBS buffer, **8** with or without light illumination for 15 min, and CORM-3, respectively. (b) Quantitative analysis of the residual wounded areas treated with PBS buffer and **8** with or without light illumination using ImageJ software. Adapted with permission from reference 64. Copyright 2020 The Royal Society of Chemistry.



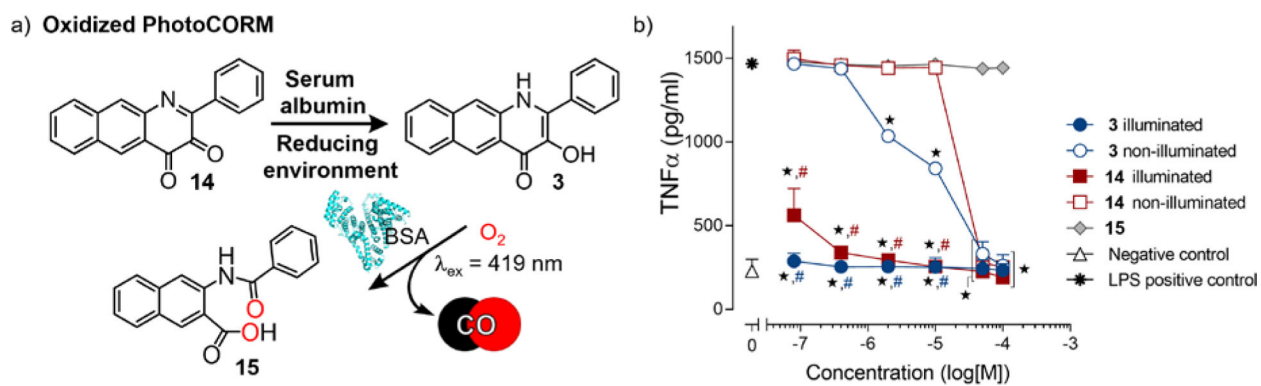


**Figure 9.** (left) Intra- and extracellular localization of **1** and **11**, respectively. (right) Anti-inflammatory effects of **1** and **11** and their CO release products (depsides) in RAW 264.7 cells under dark or visible light-induced CO release conditions. Adapted with permission from reference 47. Copyright 2019 American Chemical Society.



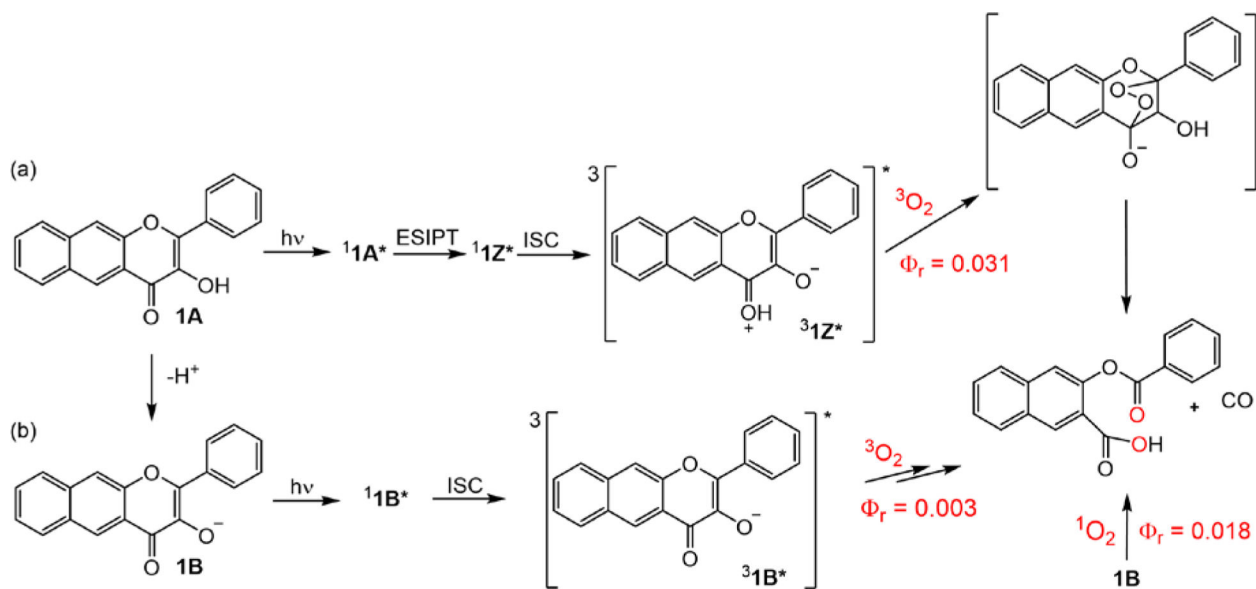
**Figure 10.**

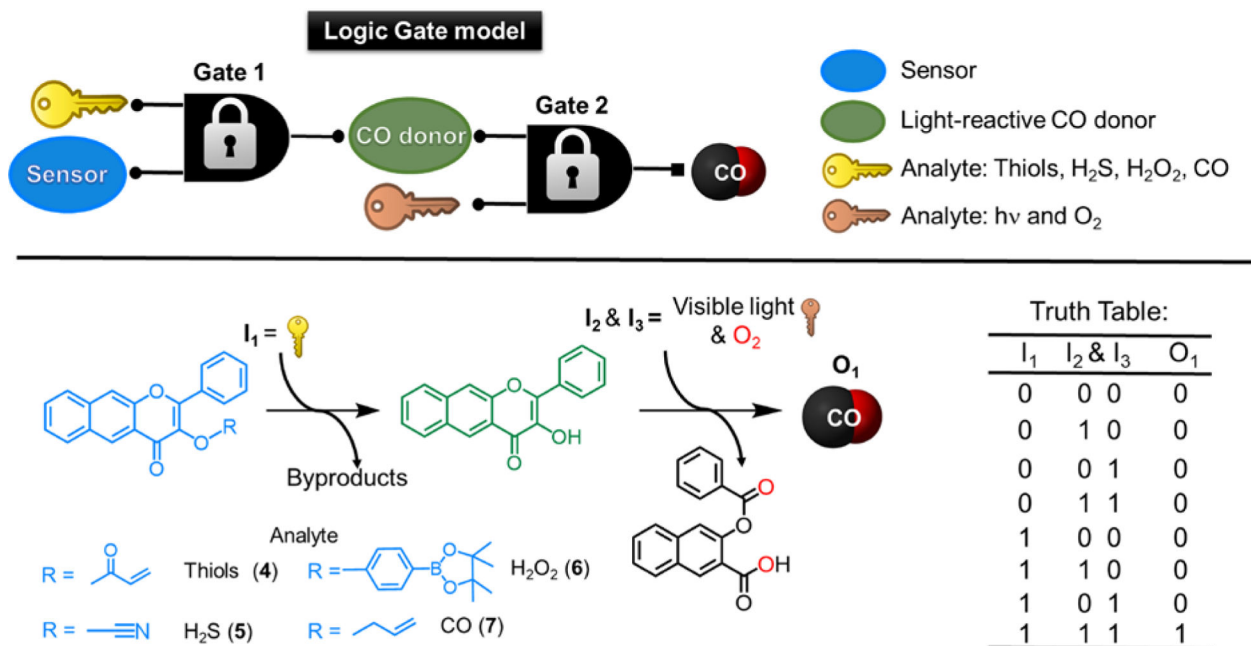
(a) Application of cytosolic **1** and mitochondria-targeted **12** in mitochondrial bioenergetics studies. (b) Confocal microscopy images showing co-localization of **12** with MTR in A549 cells. Rows 1 and 3 show cells treated with vehicle control (0.4% DMSO). Rows 2 and 4 show cells treated with **12** at 100  $\mu\text{M}$  for 4 h. Image panels depict the Hoechst nuclear stain (blue), the MitoTracker mitochondria stain (red), the CO donor **12** (green), or a merge of the three fluorescence channels. Scale bar indicates 20  $\mu\text{m}$  for rows 1 and 2. Scale bar indicates 10  $\mu\text{m}$  for rows 3 and 4. (c) Confocal images of A549 cells co-stained with **12**, MTR, and Hoechst 33342. Independent and co-localized pixels of **12** and MTR. Overlaid intensity profile of regions of interest (ROIs) in the co-stained A549 cells as indicated by the white arrows. Adapted with permission from reference 4. Copyright 2018 American Chemical Society.



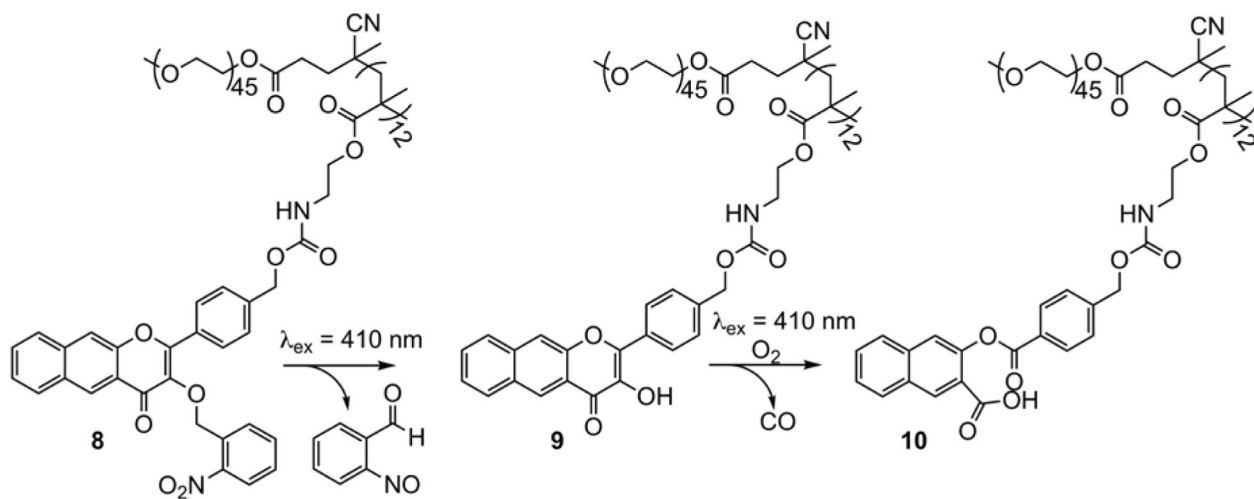
**Figure 11.**

(a) Quinolone-type photoCORM **3** along with its oxidized form (**14**, left) and CO-release product **15** (right). (b) Anti-inflammatory effects of **3**, **14** and **15** in RAW 264.7 murine macrophage cells in the presence of BSA (0.6 mM) and light (CO release in situ) or under dark conditions. Adapted with permission from reference 2. Copyright 2018 American Chemical Society.

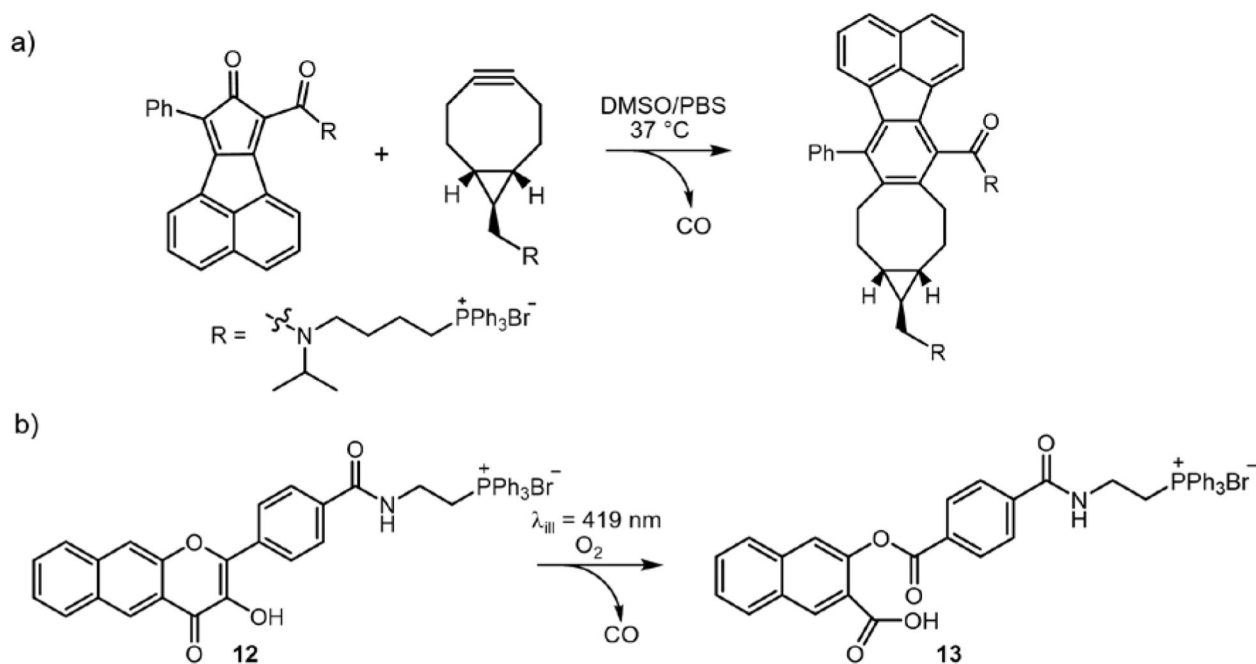
**Scheme 1.**Major reaction pathways in the photochemistry of **1** under aerobic conditions.

**Scheme 2.**

(top) Molecular AND logic gate model operation. (bottom) Analyte sensing and subsequent CO release using extended flavonol (left) and truth table based on input–output signal correlation pattern, indicating a highly regulated CO delivery (only in the sequential presence of all three inputs will CO release be enabled) (right).



**Scheme 3.**  
Visible light-induced reactivity of **8**.



**Scheme 4.**  
Mitochondria-targeted CORMs.